IGSHPA Research Track
Las Vegas, December 6-8, 2022

Transient heat transfer in ground heat exchangers under groundwater flow

Carlos Prieto **Massimo Cimmino**

ABSTRACT

An analytical solution for the transient heat transfer under groundwater flow for ground heat exchangers (GHEs) is presented. The method is an extension of the transient multipole expansion that describes the transient heat transfer as a pure conduction phenomenon inside and around a GHE including arbitrarily positioned pipes in the grout, coupling an irrotational and incompressible potential field in the ground with constant far-field velocity. The method does not rely on the supposition that groundwater flows through the GHE but instead moves around it. The method is validated against a finite element analysis model comparing the borehole wall temperature for two cases considering different single U-tube pipes position. It is shown that the thermal resistances inside the GHE do not respect the general symmetry condition $(R_{ij} \neq R_{ji}$ *and* $R_{ii} \neq R_{jj})$ *as opposed to the pure conduction problem.*

INTRODUCTION

One of the main components of ground source heat pump (GSHP) systems are ground heat exchangers (GHEs) which allow heat transfer between the building and the ground. In many applications the heat transfer between the GHE and the ground can be treated as pure heat conduction due to diffusion in the ground. However, there are cases where the impact of groundwater flow on the heat transfer process is significant. When groundwater is present, the heat transfer process is given by three effects: conduction in the ground, conduction in the groundwater and advection by groundwater. Current analytical models consider that the fluid within the ground moves unidirectionally through the GHE and not around it. This allows the classical heat conduction models such as infinite/finite line sources (ILS/FLS) (Ingersoll et al.,1948; Eskilson, 1987) and cylindrical heat source (CHS) (Carslaw and Jaeger, 1947) to be extended to their analogs when groundwater is present resulting in the moving infinite/finite line sources (MILS/MFLS) (Diao et al., 2004; Molina-Giraldo et al., 2011) and moving cylindrical heat source (MCHS) (Al-Khoury et al., 2020). These models have been used to study the response between the ground and the periphery of the GHE due to the presence of groundwater, finding that when the groundwater velocity increases, the average borehole wall temperature decreases and thus the average temperature of the circulating fluid decreases (in cooling mode) (Sutton et al., 2003; Cai et al., 2020; Wagner et al., 2013). However, how diffusion-advection of groundwater flow moving around GHE affects the heat transfer between the circulating fluid in the pipes and the borehole wall due to grout diffusion has not been studied, as well as whether the position of the pipes plays an important role in the overall heat transfer.

This paper presents a new analytical solution for the heat transfer problem that relates the groundwater flowing around the GHE by extending the transient multipole expansion for pure conduction presented by Prieto and Cimmino (2021a) in which any number of pipes could be placed inside the GHE. The groundwater model is reduced from diffusion-

Carlos Prieto (carlos.prieto@polymtl.ca) is a Ph.D. candidate and Massimo Cimmino (massimo.cimmino@polymtl.ca) is a professor of mechanical engineering at Polytechnique Montréal.

DOI: https://doi.org/10.22488/okstate.22.000031

advection to a diffusion-reaction model using a special change of variable and coefficient simplification for the reaction term. The average borehole wall temperature for two different pipe positions of a single U-tube is calculated and compared with a finite element analysis (FEA) model to validate the present solution. Thermal resistances are calculated to understand how the pipes position impacts the overall thermal response of the GHE.

MATHEMATICAL MODEL

Figure 1 shows a top view of a GHE containing two pipes ($\partial\Omega_i$, $\partial\Omega_j$) arbitrarily positioned (O_i, O_j) within the grout (Ω_1) and bounded by the borehole wall ($\partial\Omega_b$) with respect to the ground (Ω_2). The heat-carrier fluid inside the pipes has a constant temperature (T_{fi}) at each pipe i. The geometrical parameters of the GHE are the borehole wall radius (r_b) and the outer pipe radius (r_i) at each pipe i. The thermal properties of the grout and the ground are considered isotropic, constant, and homogeneous. k_b, k_s are the thermal conductivities of grout and ground, and α_b, α_s are the thermal diffusivities of the grout and ground, respectively. The ground has a constant porosity (ϵ) that allows groundwater to pass through with constant volumetric heat capacity $(\rho c_p)_f$ and thermal conductivity (k_f) through the whole ground domain. The ground is considered as a semi-infinite domain and extends to $r_e \to \infty$.

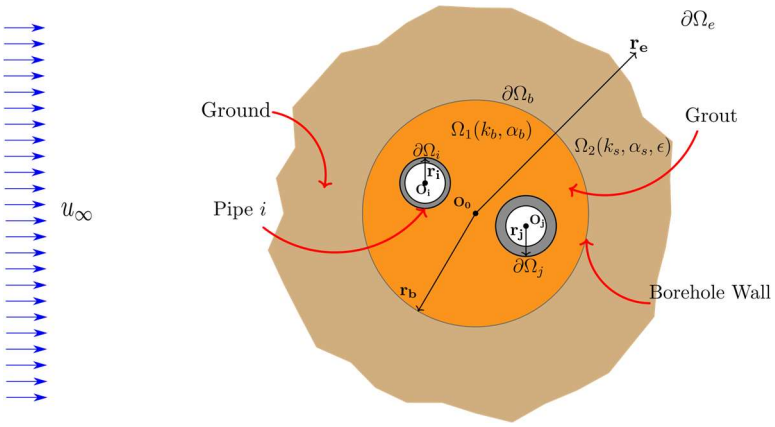

Figure 1 Domain geometry around a GHE

The transient multipole expansion of Prieto and Cimmino (2021a) is extended to describe the heat transfer phenomenon inside and outside the GHE considering groundwater flow. The original transient multipole expansion describes the heat conduction inside the periphery of the GHE for pipes arbitrarily positioned in the grout. As opposed to several existing models in the literature, the groundwater flow does not pass over the GHE but flows around it. It is assumed that the flow is incompressible and irrotational with constant far-field velocity (u_∞), resulting in a potential field.

Diffusion-advection model

The partial differential equation known as the advection-diffusion equation is used to describe the phenomenon of heat transfer in and out of the GHE for polar coordinates (ρ, ϕ) and time (t):

$$\frac{\partial T_i}{\partial t} + \frac{(\rho c_p)_f}{(\rho c_p)_i} H(\rho - r_b)\vec{u} \cdot \nabla T_i = \alpha_i \nabla^2 T_i \tag{1}$$

where $H(\rho - r_b)$ is the Heaviside function which is defined as 0 if $\rho < r_b$ and 1 otherwise, T_i is the temperature field for domain Ω_i, α_i $(= k_i/(\rho c_p)_i)$ is the thermal diffusivity for each Ω_i ($\alpha_b = \alpha_1$ and $\alpha_{s,eff} = \alpha_2$). The ground has an

effective thermal conductivity and capacity given by volume average properties defined as $k_{s,eff} = k_f\epsilon + (1-\epsilon)k_s$ and $(\rho c_p)_{s,eff} = (\rho c_p)_f \epsilon + (1-\epsilon)(\rho c_p)_s$, respectively. The velocity vector field, $\vec{u}$, is derived considering the continuity equation in the ground for a fluid moving with a density ρ_f:

$$\frac{\partial \rho}{\partial t} + \nabla \cdot (\rho_f \vec{u}) = 0 \tag{2}$$

For an incompressible and irrotational flow, Equation 2 is then a potential field $\nabla^2 \psi = 0$ which means $\vec{u} = \nabla\psi$. For a non-slip boundary condition at $\partial\Omega_b$ ($\vec{n}|_{r_b} \cdot \vec{u} = 0$), the velocity field with constant far-field velocity is then:

$$\vec{u} = u_\infty \left(1 - \frac{r_b^2}{\rho^2}\right) \cos\phi \, \widehat{e_\rho} - u_\infty \left(1 + \frac{r_b^2}{\rho^2}\right) \sin\phi \, \widehat{e_\phi} = u_\rho \widehat{e_\rho} + u_\phi \widehat{e_\phi} \tag{3}$$

where $\widehat{e_\rho}$ and $\widehat{e_\phi}$ are unitary vectors in the radial and tangential directions, respectively. The potential field is then $\psi = u_\infty \left(1 + \frac{r_b^2}{\rho^2}\right) \rho \cos\phi$.

The boundary and initial conditions of the advection-diffusion equation (Equation 1) are given by:

$$-\beta_k r_k \left.\frac{\partial T_1}{\partial \rho}\right|_{r_k} + T_1|_{r_k} = T_{fk} \text{ on } \partial\Omega_k \tag{4.1}$$

$$T_1|_{r_b} = T_2|_{r_b} \text{ on } \partial\Omega_b \tag{4.2}$$

$$-k_b \left.\frac{\partial T_1}{\partial \rho}\right|_{r_b} = -k_{s,eff} \left.\frac{\partial T_2}{\partial \rho}\right|_{r_b} + [(\rho c_p)_f u_r T_2]|_{r_b} \text{ on } \partial\Omega_b \tag{4.3}$$

$$T_2|_{r_e \to \infty} = T^0 \text{ on } \partial\Omega_e \tag{4.4}$$

$$T_i(\rho, \phi, 0) = T^0 \text{ in } \Omega_1 \cup \Omega_2 \tag{4.5}$$

Equation 4.1 corresponds to a Robin boundary condition for each pipe k with constant fluid temperature T_{fk}, where $\beta_k = 2\pi k_b R_k$ is the dimensionless fluid-to-outer wall pipe thermal resistance and R_k the fluid-to-outer wall pipe thermal resistance. Equations 4.2 and 4.3 describe the continuity conditions for temperature and heat flux, respectively. Here, it is important to mention that Equation 4.3 is different from the ones encountered in the literature since the dissipation term, $[(\rho c_p)_f u_r T_2]|_{r_b}$, is included. In this case, this term is equal to zero since the radial velocity at the borehole wall is 0 due to non-slip condition. Equations 4.4 and 4.5 are the far-field temperature and initial temperature, which are both equal to the undisturbed ground temperature T^0.

Groundwater transient multipole expansion

The resolution of the problem defined by Equations 1 and 4 is based on the methodology proposed in Prieto and Cimmino (2021a), which separates the heat transfer model as the sum of two subproblems, in this case: a) transient advection-diffusion equation with homogeneous boundary conditions ($T_{i,h}$), and b) steady-state advection-diffusion equation with non-homogenous boundary conditions ($T_{i,ss}$). The following change of variable is introduced to relate the potential field ψ with the temperature field:

$$T_{i,h} = \Gamma_{i,h} \, e^{\frac{1}{2\alpha_{s,eff}} \left(\frac{(\rho c_p)_f}{(\rho c_p)_{s,eff}}\right) H(\rho - r_b)\psi} = \Gamma_{i,h} e^{f(\rho,\phi)} \tag{5.1}$$

$$T_{i,ss} - T^0 = \Gamma_{i,ss} \, e^{\frac{1}{2\alpha_{s,eff}} \left(\frac{(\rho c_p)_f}{(\rho c_p)_{s,eff}}\right) H(\rho - r_b)\psi} = \Gamma_{i,ss} e^{f(\rho,\phi)} \tag{5.2}$$

The mathematical model for $T_{i,h}$ is reduced to a diffusion-reaction model and defined as:

$$\frac{\partial \Gamma_{i,h}}{\partial t} + H(\rho - r_b)\left(\frac{(\rho c_p)_f}{(\rho c_p)_{s,eff}}\right)^2 \left(\frac{u_\rho^2 + u_\phi^2}{4\alpha_i}\right)\Gamma_{i,h} = \alpha_i \nabla^2 \Gamma_{i,h} \tag{6.1}$$

$$-\beta_k r_k \left.\frac{\partial \Gamma_{1,h}}{\partial \rho}\right|_{r_k} + \Gamma_{1,h}|_{r_k} = 0 \text{ on } \partial\Omega_k \tag{6.2}$$

$$\Gamma_{1,h}|_{r_b} = \Gamma_{2,h}|_{r_b}\, e^{f(r_b,\theta)} \text{ on } \partial\Omega_b \tag{6.3}$$

$$-k_b \left.\frac{\partial \Gamma_{1,h}}{\partial \rho}\right|_{r_b} = -k_{s,eff} \left.\frac{\partial \Gamma_{2,h}}{\partial \rho}\right|_{r_b} e^{f(r_b,\theta)} \text{ on } \partial\Omega_b \tag{6.4}$$

$$\Gamma_{2,h}|_{r_e \to \infty} = 0 \text{ on } \partial\Omega_e \tag{6.5}$$

$$\Gamma_{i,h}(\rho, \phi, 0) = (T^0 - T_{i,ss})/e^{f(\rho,\phi)} \quad \text{in } \Omega_1 \cup \Omega_2 \tag{6.6}$$

For $T_{i,ss}$, the problem is described as:

$$H(\rho - r_b)\left(\frac{(\rho c_p)_f}{(\rho c_p)_{s,eff}}\right)^2 \left(\frac{u_\rho^2 + u_\phi^2}{4\alpha_i}\right)\Gamma_{i,ss} = \alpha_i \nabla^2 \Gamma_{i,ss} \tag{7.1}$$

$$-\beta_k r_k \left.\frac{\partial \Gamma_{1,ss}}{\partial \rho}\right|_{r_k} + \Gamma_{1,ss}|_{r_k} = T_{fk} - T^0 \text{ on } \partial\Omega_k \tag{7.2}$$

$$\Gamma_{1,ss}|_{r_b} = \Gamma_{2,ss}|_{r_b}\, e^{f(r_b,\phi)} \text{ on } \partial\Omega_b \tag{7.3}$$

$$-k_b \left.\frac{\partial \Gamma_{1,ss}}{\partial \rho}\right|_{r_b} = -k_{s,eff} \left.\frac{\partial \Gamma_{2,ss}}{\partial \rho}\right|_{r_b} e^{f(r_b,\phi)} \text{ on } \partial\Omega_b \tag{7.4}$$

$$\Gamma_{2,ss}|_{r_e \to \infty} = 0 \text{ on } \partial\Omega_e \tag{7.5}$$

An approximation of the reaction coefficient $u_\rho^2 + u_\phi^2 = u_\infty^2\left(1 - \frac{2r_b^2}{\rho^2}\cos 2\phi + \frac{r_b^4}{\rho^4}\right) \approx K_{gw} u_\infty^2$ is proposed to simplify the model presented in Equations 6.1 and 7.1. This approximation is valid since $u_r^2 + u_\theta^2$ has a maximum value of $4u_\infty^2$ for $\rho = r_b, \phi = (2n+1)\pi$ for $n \in Z$ and a minimum value of 0 for $\rho = r_b, \phi = n\pi$. Moreover, when ρ is sufficiently large when compared with r_b, the value is u_∞^2. It was found that $K_{gw} = 1.6$ produces a good approximation.

Equation 6.1 has a similar structure to those expressed in Prieto and Cimmino (2021a). Thus, assuming that $\Gamma_{i,h}$ is spatiotemporally separable as $\Gamma_{i,h} = X_i(\rho, \phi)\tau(t)$ results in a Sturm-Liouville problem with $\tau(t) = \exp\left(-\left(\lambda_i^j\right)^2 \alpha_i t\right)$ for unique j eigenvalues for each domain i denoted as λ_i^j. The continuity condition requires that $\alpha_1\left(\lambda_1^j\right)^2 = \alpha_2\left(\lambda_2^j\right)^2$ must hold for all time t. Therefore, the problem $X_i(\rho, \phi)$, defined as the Helmholtz equation for the interior of the GHE (i.e. X_1), has the same formulation as that of the transient multipole expansion for a point $\mathbf{x}$ with coordinates related to a particular pipe center O_k given by $\mathbf{x_k} = (\rho_k, \phi_k)$ and for the GHE center $\mathbf{x_0} = (\rho_0, \phi_0)$:

$$X_1(\mathbf{x}; \lambda_1^j) = \sum_{l=-M}^{M} \gamma_l^0 J_l(\lambda_1^j \rho_0) e^{il\phi_0} + \sum_{k=1}^{N}\sum_{l=-M}^{M} \gamma_{l,j}^k H_l^{(1)}(\lambda_1^j \rho_k) e^{il\phi_k} \tag{8}$$

For the ground domain, the expansion for X_2 is slightly different:

$$X_2(\mathbf{x}; \lambda_2^j) = \sum_{l=-M}^{M} \delta_l^0 H_l^{(1)}(\sigma_j \rho_0)\, e^{il\phi_0} \tag{9}$$

where $\sigma_j^2 = \left(\lambda_2^j\right)^2 - u_\infty^2\left(\frac{K_{gw}}{4\alpha_2^2}\right)\left(\frac{(\rho c_p)_f}{(\rho c_p)_{s,eff}}\right)^2$, and J and $H^{(1)}$ are the first kind Bessel and Hankel functions, respectively. The calculation of the eigenvalues is done by means of singular value decomposition (SVD), as done by Prieto and Cimmino (2021a). The coefficients $\gamma^0, \gamma^k, \delta^0$ are the coefficients that match the boundaries and calculated for each eigenvalue.

The full solution for $\mathrm{T}_{i,h}$ is given by a Fourier-Bessel expansion:

$$\mathrm{T}_{i,h}(\mathrm{x},\mathrm{t}) = \sum_{\mathrm{j}=1}^{\infty} C_j \ \mathrm{X_i}\left(\mathrm{x};\lambda_{\mathrm{i}}^{\mathrm{j}}\right)\mathrm{e}^{-\left(\lambda_{\mathrm{i}}^{\mathrm{j}}\right)^2 \alpha_{\mathrm{i}}\, \mathrm{t}+\mathrm{f}(\rho,\phi)} \tag{10}$$

where C_j are in this case:

$$C_j = \frac{\frac{k_b}{\alpha_b}\int_{\Omega_1}(T^0-T_{2,ss})\overline{X_1}d\Omega_1+\frac{k_{s,eff}}{\alpha_{s,eff}}\int_{\Omega_2}(T^0-T_{2,ss})\overline{X_2}e^{2f(r_b,\phi)-f(\rho,\phi)}d\Omega_2}{\frac{k_b}{\alpha_b}\int_{\Omega_1}X_1\overline{X_1}d\Omega_1+\frac{k_{s,eff}}{\alpha_{s,eff}}\int_{\Omega_2}X_2\overline{X_2}e^{2f(r_b,\phi)}d\Omega_2} \tag{11}$$

The coefficients expressed in Equation 11 are obtained by means of the quasi-orthogonal conditions of the Sturm-Liouville problem and using Green's second identity.

Similarly, for Equation 7.1, the same procedure is done. For the grout, the same multipole expansion presented in Prieto and Cimmino (2021a) is used:

$$\Gamma_{1,ss} = \alpha_0 + \sum_{m=1}^{h}\left[\alpha_m\left(\frac{\rho_0}{r_{max}}\right)\cos(m\phi_0) + \beta_m\left(\frac{\rho_0}{r_{max}}\right)\sin(m\phi_0)\right] + \sum_{k=1}^{N}\left\{\gamma_0^k \ln\rho_k + \sum_{m=1}^{h}\left[\gamma_m^k\left(\frac{\rho_k}{r_{min}}\right)\cos(m\phi_k) + \delta_{\mathrm{m}}^{\mathrm{k}}\left(\frac{\rho_{\mathrm{k}}}{\mathrm{r}_{min}}\right)\sin(m\phi_k)\right]\right\} \tag{12}$$

For the ground, the multipole expansion is given by:

$$\Gamma_{2,ss} = \sum_{l=-h}^{h}\delta_l^0 K_l\left(u_\infty\left(\frac{\sqrt{K_{gw}}}{2\alpha_2}\right)\left(\frac{(\rho c_p)_f}{(\rho c_p)_{s,eff}}\right)\rho_0\right)e^{il\phi_0} \tag{13}$$

where K is the modified Bessel function of the second kind of order l and $\alpha, \beta, \gamma, \delta$ are the coefficients that match the boundaries which are different from the homogenous problem.

RESULTS

The average borehole wall temperature (T_b) is evaluated using the present method and FEA for 4 different far field velocities: $u_\infty = 0, 10^{-6}, 10^{-5}, 10^{-4}\ m/s$. Two cases are studied, with the same thermal properties and geometrical parameters shown in Table 1 but with different positioning of the pipes: (I) the pipes are positioned at $O_1(-0.05,0)$, $O_2(0.05,0)$, and (II) $O_1(0,0.05)$, $O_2(0,-0.05)$. The FEA model for both cases is composed of 5504 nodes and 9906 triangular elements (second order Lagrange elements) with $r_e = 55\ m$. The parameters for the multipole expansion are set to $M = 14$ and $h = 30$, doubling those shown in Prieto and Cimmino (2021a) due to the exponential term in the continuity conditions (Equations 6.3-6.4 and 7.3-7.4), and the first 100 eigenvalues are used.

TABLE 1. GHE PARAMETERS

Parameter	Value	Parameter	Value
Grout thermal conductivity	$k_b = 0.81\ W/(mK)$	Borehole radius	$r_b = 0.075\ m$
Grout thermal diffusivity	$\alpha_b = 2.13 \times 10^{-7} m^2/s$	U-tube pipe outer radius	$r_k = 0.021082\ m$
Ground thermal conductivity	$k_s = 2.4\ W/(mK)$	Dimensionless fluid-to-pipe thermal resistance	$\beta_k = 0.480281$
Ground thermal diffusivity	$\alpha_s = 1.2 \times 10^{-6}\ m^2/s$	Undisturbed ground temperature	$T^0 = 10\ ℃$
Groundwater thermal conductivity	$k_f = 0.48\ W/(mK)$	Porosity	$\epsilon = 0.2$
Groundwater thermal capacity	$(\rho c_p)_f = 4.2 \times 10^6\ J/(m^3K)$	Shank spacing	$e = 0.1\ m$

Figure 2 shows the average borehole wall temperature calculated by the present method (dotted line) and the FEA

method (solid line) for cases I and II for a period of 60000 s with a time-step equal to 60s considering the four different far-field velocities with fluid temperatures equal to $T_{f1} = T_{f2} = 20\ °C$ for both cases. Figure 2 also shows temperature contours for the final simulation time with $u_\infty = 10^{-5}\ m/s$. As expected, when the far-field velocity increases the average borehole wall temperature decreases and reaches the quasi-steady-state condition earlier. The maximum absolute differences between the proposed method and the FEA appear at approximately 180 h (10740 s) with values of $0.105, 0.115, 0.117, 0.061°C$ for case I and $0.090, 0.103, 0.106, 0.024°C$ for Case II, for each far-field velocity $u_\infty = 0,\ 10^{-6}, 10^{-5}, 10^{-4}\ m/s$, respectively. At the final simulation time, the maximum difference between the proposed method and the FEA is $0.010°C$ for case I with $u_\infty = 10^{-6}\ m/s$. The main reason for this discrepancy is the simplification in Equations 6.1 and 7.1 for the reaction coefficient. The relatively small errors show that the coefficient K_{gw} can be used to successfully simplify the problem without significant loss of accuracy. Figure 2 also shows that the borehole wall temperatures are different in cases I and II for the same far-field velocity when $u_\infty \geq 10^{-5}\ m/s$. This implies that, under groundwater flow, the orientation of the U-tube influences the internal thermal resistances.

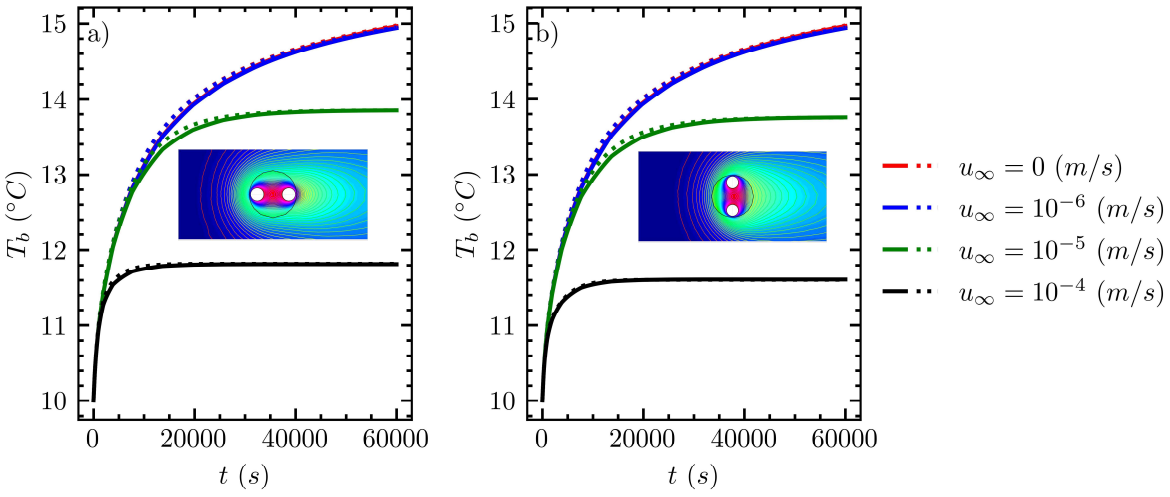

Figure 2 Average borehole wall temperature comparison between FEA (continuous line) and present method (discontinuous line) for 4 different far-field velocities: a) Case I and b) Case II

The internal thermal resistances are defined by:

$$T_{f1} - T_b = R_{11}q_1 + R_{12}q_2 \tag{14.1}$$

$$T_{f2} - T_b = R_{21}q_1 + R_{22}q_2 \tag{14.2}$$

where $q_k = \left(T_{fk} - \overline{T_1|_{r_k}}\right)/R_k$ is the heat flow at each pipe k, with $\overline{T_1|_{r_k}}$ the average outer-wall pipe temperature. Internal thermal resistances are generally symmetrical ($R_{11} = R_{22}$ and $R_{12} = R_{21}$) in the absence of groundwater flow when symmetrical positioned pipes are considered. To estimate the thermal resistances, two pairs of arbitrary constant fluid temperatures for both pipes are used to solve the system of equations defined by Equations 14. Figures 3 and 4 show the thermal resistances defined in Equation 14 for the two cases, with Figures 3a and 4a corresponding to $u_\infty = 0\ m/s$. The internal thermal resistances are symmetrical for this velocity. The thermal resistances calculated with the multipole method developed by Claesson and Hellström (2011) for the quasi-steady-state condition (conduction problem) are $R_{11} = R_{22} = 0.291\ mK/W$ and $R_{12} = R_{21} = -0.029\ mK/W$ for both cases. Comparing these

resistances with the final simulation time shown in Figure 3a and Figure 4a, the thermal resistances are $R_{11} = R_{22} = 0.285\ mK/W$ and $R_{12} = R_{21} = -0.027\ mK/W$. As expected, thermal resistances are symmetrical and are in good agreement with the classical multipole method. There are small differences between the multipole method and the transient multipole expansion since the transient multipole has not reached steady state. When $t \to \infty$, the thermal resistances approach to those calculated by Claesson and Hellström (2011).

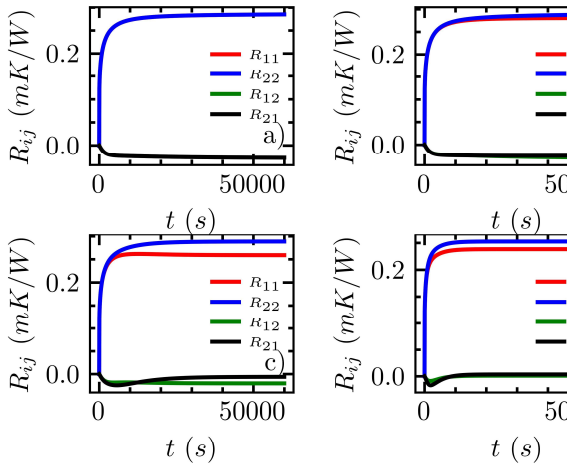

Figure 3 Internal thermal resistances for case I with different far-field velocities: a) $u_\infty = 0\ m/s$, b) $u_\infty = 10^{-6}\ m/s$, c) $u_\infty = 10^{-5}\ m/s$ and d) $u_\infty = 10^{-4}\ m/s$

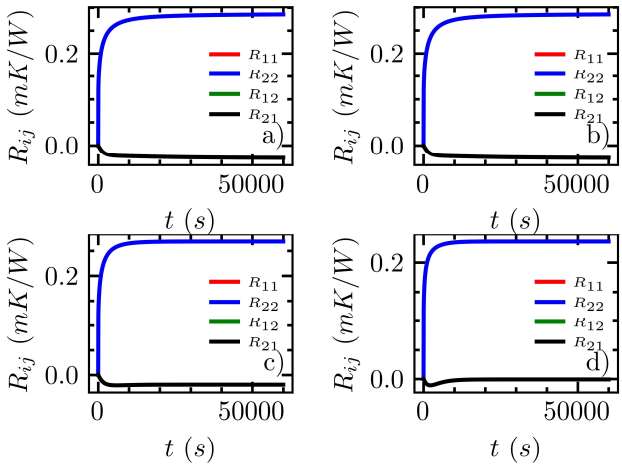

Figure 4 Internal thermal resistances for case II with different far-field velocities: a) $u_\infty = 0\ m/s$, b) $u_\infty = 10^{-6}\ m/s$, c) $u_\infty = 10^{-5}\ m/s$ and d) $u_\infty = 10^{-4}\ m/s$

As shown on Figures 3b-d for case I, the thermal resistances decrease when the far-field velocity increases, and the symmetry tends to break down at higher far-field velocities. This is not the case on Figures 4b-d for case II where the symmetry holds at all far-field velocities. At the final time, the values of the thermal resistances are $R_{11} = 0.281, 0.259, 0.239, R_{22} = 0.289, 0.289, 0.253, R_{12} = -0.029, 0.020, 0.0, R_{21} = -0.024, -0.006, 0.003$ for case I, and $R_{11} = R_{22} = 0.285, 0.267, 0.234, R_{21} = R_{21} = -0.027, -0.02, -0.001$ for case II, respectively, for each far-field velocity $u_\infty = 10^{-6}, 10^{-5}, 10^{-4}\ m/s$.

On Figures 3c-d and 4c-d, it is observed that the resistances R_{11} and R_{22} are not equal for case I, however they are equal for case II. This interesting result shows that even though the pipes are symmetrically distributed within the GHE, the symmetry condition does not hold in general. The fact that case II does present symmetry is because the far-field velocity is perpendicular to the spacing between the pipes. This allows using Green's identities to show that for this case the symmetry condition holds. It is also interesting to observe the behavior of resistances R_{12} and R_{21} for both cases I and II. Figures 3d and 4d show that these resistances tend to 0 as the velocity increases. In both cases, this behaviour on thermal resistances is explained in that the heat transfer is due to heat exchange between each pipe and the borehole wall rather than the pipes transferring heat to each other, therefore the groundwater is dissipating heat from the pipes.

CONCLUSION

A new analytical method for the study of conduction-advection heat transfer inside and around of a GHE was presented. The method allows including a potential field in the ground flowing around the GHE, in this case incompressible and irrotational. No simplification inside the GHE is made, allowing to place different pipe positions. Also, when posing

the complete mathematical model, a new boundary condition is considered in Equation 4.3 which takes into account the energy dissipation by means of the groundwater advection.

As a first validation, the method was compared with a high-fidelity FEA simulation, which showed that the present method possesses good agreement despite making an approximation in the reduction of the diffusion-reaction problem by introducing a K_{gw} coefficient. With this new analytical method, it was shown that the position of the pipes slightly changes the temperature around the GHE. The observation of the temperature around the borehole wall showed that the thermal resistances coming from the linear conduction problem inside the GHE are not symmetric ($R_{ii} \neq R_{jj}$ and $R_{ij} \neq R_{ji}$). It was found that when the groundwater velocity is sufficiently large, the heat transfer problem is one-dimensional, meaning that to calculate the heat flux of each pipe it is sufficient to know the temperature of each pipe and the average borehole temperature as $R_{ij} \to 0$ for $i \neq j$.

With these results, the use of methods such as thermal resistance capacitance (TRC) methods should be revisited when including groundwater flow, as the delta-circuit is not always valid. Extending the method from 2D to 3D including thermal interactions between boreholes and time-dependent fluid temperatures could be done using a segmented MFLS solution (Cimmino and Baliga, 2019) and a modified equivalent borehole method (Prieto and Cimmino, 2021b) with a coefficient updating scheme as done in Prieto and Cimmino (2021a, 2022).

ACKNOWLEDGMENTS

This study is funded by the Natural Sciences and Engineering Research Council of Canada (NSERC) [grant number: RGPIN-2018-04471].

REFERENCES

Al-Khoury, R., N. Bnilam, M. Arzanfudi and S. Saeid. 2020. *A spectral model for a moving cylindrical heat source in a conductive-convective domain.* International Journal of Heat and Mass Transfer 163: 120517.

Cai, S., X. Li, M. Zhang, J. Fallon, K. Li and T. Cui. 2020. *An analytical full-scale model to predict thermal response in boreholes with groundwater advection.* Applied Thermal Engineering 168: 114828

Carslaw, H. S. and J. C. Jaeger. 1947. *Conduction of heat in solid.* Oxford: Claremore Press.

Cimmino, M. and B. R. Baliga. 2019. *A hybrid numerical-semi-analytical method for computer simulations of groundwater flow and heat transfer in geothermal borehole fields.* International Journal of Thermal Sciences 142: 366–378.

Claesson, J. and G. Hellström. 2011. *Multipole method to calculate borehole thermal resistances in a borehole heat exchanger*. HVAC&R Research 17(6): 895-911.

Diao, N., Q. Li and Z. Fang. 2004. *Heat transfer in ground heat exchangers with groundwater advection*. International Journal of Thermal *Sciences* 43 (12):1203-1211.

Eskilson, P. 1987. *Thermal analysis of heat extraction boreholes*. Ph.D. Thesis. Lund university, Lund, Sweden.

Ingersoll, L. R., O. J. Zobel and A. C. Ingersoll. 1948. *Heat conduction with engineering and geological applications*. Heat Conduction with Engineering and Geological Applications:278.

Molina-Giraldo, N., P. Blum, K. Zhu, P. Bayer and Z. Fang. 2011. *A moving finite line source model to simulate borehole heat exchangers with groundwater advection.* International Journal of Thermal Sciences 50(12): 2506-2513

Prieto, C. and M. Cimmino. 2021a. *Transient multipole expansion for heat transfer in ground heat exchangers*. Science and Technology for the Built Environment 27(3): 253-270

Prieto, C. and M. Cimmino. 2021b. *Thermal interactions in large irregular fields of geothermal boreholes: the method of equivalent boreholes*. Journal of Building Performance Simulation 14(4): 446-460.

Prieto, C. and M. Cimmino. 2022. *Semi-Analytical Method for 3D Transient Heat Transfer in Thermally Interacting Fields of Ground Heat Exchangers*. Thermo 2(3): 171-199.

Sutton, M. G., D. W. Nutter and R. J. Couvillion. 2003. *A ground resistance for vertical bore heat exchangers with groundwater flow*. Journal of Energy Resources Technology 125(3): 183-189.

Wagner, V., P. Blum, M. Kübert and P. Bayer. 2013. *Analytical approach to groundwater-influenced thermal response tests of grouted borehole heat exchangers*. Geothermics 46:22-31.